Effects of sampling and limited data in optical tomography

Vadim A. Markel[a)] and John C. Schotland[b)]
Department of Radiology, Washington University, St. Louis, Missouri 63110

(Received 11 February 2002; accepted for publication 28 May 2002)

We consider the image reconstruction problem for optical tomography in the transmission geometry. We investigate the effects of sampling and limited data on this inverse problem and derive an explicit inversion which is computationally efficient and stable in the presence of noise. © *2002 American Institute of Physics.* [DOI: 10.1063/1.1495543]

The propagation of near-infrared light in many biological tissues is characterized by strong multiple scattering and relatively weak absorption.[1] Under these conditions, the transport of light can be regarded as occurring by means of diffusing waves.[2] There has been considerable recent interest in the use of such waves for medical imaging.[3] The physical problem under consideration consists of recovering the optical properties of the interior of an inhomogeneous medium from measurements taken on its surface. A fundamental question of substantial practical importance concerns the impact of limited data on this inverse scattering problem.[4–6] This question arises since it is often not possible to measure all the data which is necessary to guarantee uniqueness or stability of a solution to the inverse problem. A related question is how to recover the properties of the medium with a certain spatial resolution. Hence, it is important to understand the effects of sampling of the measured data on the quality of reconstructed images.

In this letter, we consider the linearized inverse problem of optical diffusion tomography with sampled and limited data in the slab geometry. In this geometry, which is often used in optical mammography, measurements are taken with N sources located on one face of the slab and N detectors located on the opposite face. In addition, we assume that the sources and detectors are placed on a square lattice with lattice spacing h. Under these assumptions, we show that it is possible to obtain a suitably defined solution to the inverse problem in the form of an explicit inversion formula. An important consequence of this result is that the fundamental limit of resolution in the transverse direction is the lattice spacing h. The resolution in the depth direction is a more delicate matter and is determined by numerical precision and the level of noise in the measurements. Resolution is further controlled by the size of the window $W=Nh$ on which the data is taken.

We begin by considering the propagation of diffuse light in the slab geometry. We work in the frequency domain and assume that the sources are harmonically modulated at the frequency ω. The detectors are assumed to yield measurements of the oscillatory part of the transmitted intensity. For simplicity, we restrict our attention to the case in which the slab is characterized by an inhomogeneous optical absorption coefficient $\alpha(\mathbf{r})$ and a diffusion constant D_0. The change in intensity of transmitted light due to fluctuations in $\alpha(\mathbf{r})$ can be obtained from the integral equation[7,8]

$$\phi(\boldsymbol{\rho}_s,\boldsymbol{\rho}_d)=\int \Gamma(\boldsymbol{\rho}_s,\boldsymbol{\rho}_d;\mathbf{r})\,\delta\alpha(\mathbf{r})d^3r, \tag{1}$$

where the *data function* $\phi(\boldsymbol{\rho}_s,\boldsymbol{\rho}_d)$ is proportional to the change in intensity relative to a reference medium with absorption α_0, $\delta\alpha(\mathbf{r})=\alpha(\mathbf{r})-\alpha_0$, and $\boldsymbol{\rho}_s$ and $\boldsymbol{\rho}_d$ denote the transverse coordinates of a point source on the plane $z=0$ and a point detector on the plane $z=L$. The kernel $K(\boldsymbol{\rho}_s,\boldsymbol{\rho}_d;\mathbf{r})$ is expressed in terms of the Green's functions for the diffusion equation in the reference medium and can be expressed as the Fourier integral

$$\Gamma(\boldsymbol{\rho}_s,\boldsymbol{\rho}_d;\mathbf{r})=\int \frac{d^2q_s d^2q_d}{(2\pi)^4}\kappa(\mathbf{q}_s,\mathbf{q}_d;z) \times\exp[i(\mathbf{q}_s-\mathbf{q}_d)\cdot\boldsymbol{\rho}-i(\mathbf{q}_s\cdot\boldsymbol{\rho}_s-\mathbf{q}_d\cdot\boldsymbol{\rho}_d)], \tag{2}$$

where $\mathbf{r}=(\boldsymbol{\rho},z)$. General expressions for the functions κ are given in Ref. 9 and depend upon the nature of the boundary conditions obeyed by the Green's function. Here, we consider absorbing boundaries in which case

$$\kappa(\mathbf{q}_s,\mathbf{q}_d;z)=\left(\frac{l^*}{D_0}\right)^2\frac{\sinh[Q(\mathbf{q}_s)(L-z)]\sinh[Q(\mathbf{q}_d z)]}{\sinh[Q(\mathbf{q}_s)L]\sinh[Q(\mathbf{q}_d)L]}, \tag{3}$$

where $Q(\mathbf{q})=(q^2+k^2)^{1/2}$, k is the (generally, complex) diffuse wave number given by $k^2=(\alpha_0-i\omega)/D_0$, and l^* is the transport mean free path.

We now turn to the derivation of the inversion formula for sampled data. The approach we will follow is a modification of the method of Refs. 10 and 11 in which an inversion formula was obtained for the case of *complete data*, that is continuously measured over the infinite faces of the slab. Note that although the complete-data inversion formula, in principle, provides an exact solution to the linearized inverse problem, it is only the starting point for developing accurate numerical algorithms. To proceed, we introduce the Fourier-transformed data function which is defined by

$$\tilde{\phi}(\mathbf{u},\mathbf{v})=\sum_{\boldsymbol{\rho}_s,\boldsymbol{\rho}_d}\phi(\boldsymbol{\rho}_s,\boldsymbol{\rho}_d)e^{i(\mathbf{u}\cdot\boldsymbol{\rho}_s+\mathbf{v}\cdot\boldsymbol{\rho}_d)}, \tag{4}$$

where the sum over $\boldsymbol{\rho}_s$ and $\boldsymbol{\rho}_d$ is carried out over all lattice vectors and $\mathbf{u}$, $\mathbf{v}$ are in the first Brillouin zone (FBZ) of the lattice. Making use of the identity $\Sigma_{\boldsymbol{\rho}}\exp(i\mathbf{u}\cdot\boldsymbol{\rho})=(2\pi/h)^2\Sigma_{\mathbf{s}}\delta(\mathbf{u}-\mathbf{s})$, where $\mathbf{u}$ denotes a reciprocal lattice vector, and applying the definition (4) to Eqs. (1) and (2), we obtain

[a)]Electronic mail: vmarkel@altai.wustl.edu
[b)]Electronic mail: jcs@ee.wustl.edu

 © 2002 American Institute of Physics
Downloaded 12 Aug 2002 to 128.252.91.125. Redistribution subject to AIP license or copyright, see http://ojps.aip.org/aplo/aplcr.jsp

$$\tilde{\phi}(\mathbf{u},\mathbf{v}) = \frac{1}{h^4}\sum_{\mathbf{s},\mathbf{s}'}\int_0^L \kappa(\mathbf{u}+\mathbf{s},-\mathbf{v}-\mathbf{s}';z) \times \delta\tilde{\alpha}(\mathbf{u}+\mathbf{v}+\mathbf{s}+\mathbf{s}',z)dz, \tag{5}$$

where

$$\delta\tilde{\alpha}(\mathbf{q},z) \equiv \int \delta\alpha(\boldsymbol{\rho},z)\exp(i\mathbf{q}\cdot\boldsymbol{\rho})d^2\rho, \tag{6}$$

and $\mathbf{s}$ and $\mathbf{s}'$ are reciprocal lattice vectors. To avoid the use of redundant data, we multiply both sides of Eq. (5) by the function $\chi(\mathbf{u},\mathbf{v})$ which is unity inside the FBZ and zero outside.[12] Then, we define a new function $\psi(\mathbf{q},\mathbf{p}) = h^4\chi(\mathbf{q}/2+\mathbf{p},\mathbf{q}/2-\mathbf{p})\tilde{\phi}(\mathbf{q}/2+\mathbf{p},\mathbf{q}/2-\mathbf{p})$ where $\mathbf{p}$ and $\mathbf{q}$ range over all space. Making use of this definition and the change of variables $\mathbf{s}+\mathbf{s}'=\mathbf{s}_1$ and $\mathbf{s}-\mathbf{s}'=\mathbf{s}_2$, we find that

$$\psi(\mathbf{q},\mathbf{p}) = \chi(\mathbf{q}/2+\mathbf{p},\mathbf{q}/2-\mathbf{p}) \times \sum_{\mathbf{s}_1}\sum_{\mathbf{s}_2\in\sigma(\mathbf{s}_1)}\int_0^L dz\,\kappa\left(\mathbf{p}+\frac{\mathbf{s}_1+\mathbf{s}_2+\mathbf{q}}{2}, \mathbf{p}+\frac{\mathbf{s}_1-\mathbf{s}_2-\mathbf{q}}{2};z\right)\delta\tilde{\alpha}(\mathbf{q}+\mathbf{s}_1,z), \tag{7}$$

where $\sigma(\mathbf{s}_1)$ is the set of values that $\mathbf{s}_2$ can take for a fixed $\mathbf{s}_1$. Following the general method of Refs. 10 and 11, we treat the variable $\mathbf{q}$ as continuous and $\mathbf{p}$ as discrete with $\mathbf{p}\in\{\mathbf{p}_1,\ldots,\mathbf{p}_M\}$, and define

$$F_m(\mathbf{q}) = \psi(\mathbf{q},\mathbf{p}_m), \tag{8}$$

$$K_m(\mathbf{q},\mathbf{s}_1;z) = \chi(\mathbf{q}/2+\mathbf{p}_m,\mathbf{q}/2-\mathbf{p}_m) \times \sum_{\mathbf{s}_2\in\sigma(\mathbf{s}_1)}\kappa\left(\mathbf{p}+\frac{\mathbf{s}_1+\mathbf{s}_2+\mathbf{q}}{2},\mathbf{p}+\frac{\mathbf{s}_1-\mathbf{s}_2-\mathbf{q}}{2};z\right), \tag{9}$$

so that the integral Eq. (7) becomes

$$F_m(\mathbf{q}) = \sum_{\mathbf{s}_1}\int_0^L K_m(\mathbf{q},\mathbf{s}_1;z)\delta\tilde{\alpha}(\mathbf{q}+\mathbf{s}_1,z)dz. \tag{10}$$

The pseudoinverse solution to this one-dimensional integral equation is given by

$$\delta\tilde{\alpha}(\mathbf{q}+\mathbf{s},z) = \sum_{m,l} K_m^*(\mathbf{q},\mathbf{s};z)M_{ml}^{-1}(\mathbf{q})F_l(\mathbf{q}), \tag{11}$$

where

$$M_{lm}(\mathbf{q}) = \sum_{\mathbf{s}}\int_0^L K_m(\mathbf{q},\mathbf{s};z)K_l^*(\mathbf{q},\mathbf{s};z)dz. \tag{12}$$

If $\mathbf{q}\in$ FBZ and $\mathbf{s}$ takes all possible values in the reciprocal lattice, then Eq. (11) defines all possible transverse Fourier components of $\delta\alpha(\mathbf{r})$, which can be now obtained by inverting Eq. (6). We thus arrive at the main result of this letter, which is the required inversion formula for $\delta\alpha$:

$$\delta\alpha(\mathbf{r}) = \int_{\mathrm{FBZ}}\frac{d^2q}{(2\pi)^2}\exp(-i\mathbf{q}\cdot\boldsymbol{\rho})\sum_{m,l} P_m^*(\mathbf{q},\mathbf{r})M_{ml}^{-1}(\mathbf{q})F_l(\mathbf{q}), \tag{13}$$

where

$$P_m(\mathbf{q},\mathbf{r}) = \sum_{\mathbf{s}}\exp(i\mathbf{s}\cdot\boldsymbol{\rho})K_m(\mathbf{q},\mathbf{s};z). \tag{14}$$

Several comments on the inversion formula (13) are necessary. For the case of complete data, the inverse problem is overdetermined. This should be contrasted with the case of discrete, sampled data in which the inverse problem is underdetermined. In either case, the solution we have constructed to the inverse problem is the minimum L^2 norm solution to the integral Eq. (7). If, however, $\delta\alpha$ is restricted to the subspace of transversely band-limited functions, the inverse problem with discrete data is no longer underdetermined and the sum over $\mathbf{s}$ in Eqs. (14) and (12) may be truncated. Thus, the inversion formula produces the best (in the sense of minimizing L^2 norm) transversely band-limited approximation to $\delta\alpha$ that is consistent with the lattice on which the data function is sampled.

Multiple factors control the spatial resolution of images reconstructed using the inversion formula (13). Numerical stability is an important factor determining resolution and is influenced by the existence of small singular values of M. Accordingly, M^{-1} must be regularized by setting

$$M^{-1} = \sum_{m=1}^{M}\Theta(\sigma_m^2-\epsilon)\sigma_m^{-2}|c_m\rangle\langle c_m|, \tag{15}$$

where $|c_m\rangle$ and σ_m^2 are the eigenvectors and eigenvalues of M, ϵ is a small regularization parameter, and $\Theta(x)$ is the unit step function. The minimum value of ϵ for which reconstruction is numerically stable is defined by noise, and in the absence of noise by numerical precision. For sufficiently small ϵ, the transverse resolution is defined only by the size of the FBZ in integration (13) and, therefore, is equal to h. In contrast, the depth resolution always depends on ϵ and in the absence of noise is determined by numerical precision. Resolution can further decrease when the window size W is finite. Indeed, the inversion formula derived here uses data on an infinite lattice. In the case of finite W, $\phi(\boldsymbol{\rho}_s,\boldsymbol{\rho}_d)$ is not known for all values of its arguments. Therefore, Fourier transformation of the data function according to Eq. (4) can be carried out only approximately, by truncating the infinite sum. The effect of this truncation is to introduce additional systematic errors in $F_l(\mathbf{q})$. Reconstruction using such data will require an increased regularization parameter and will have lower resolution.

To illustrate the nature of the resolution for different values of h and W, we have performed numerical simulations using continuous wave (cw) data ($\omega=0$). The object to be imaged is a small point absorber of the form $\delta\alpha(\mathbf{r}) = a\,\delta(\mathbf{r}-\mathbf{r}_0)$, located between the two measurement planes at $\mathbf{r}_0=(0,0,L/2)$. Integration over $\mathbf{q}$ in Eq. (13) is performed by discretizing the integration region (41×41 discrete values

Downloaded 12 Aug 2002 to 128.252.91.125. Redistribution subject to AIP license or copyright, see http://ojps.aip.org/aplo/aplcr.jsp

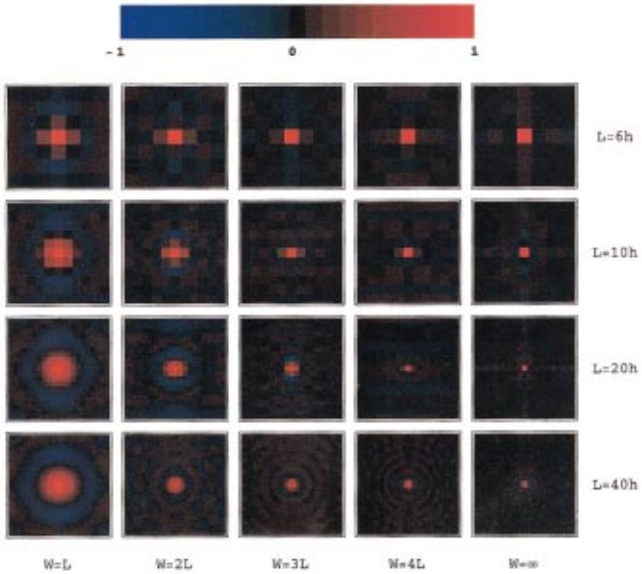

FIG. 1. (Color) Transverse resolution for different values of parameters h and W.

of $\mathbf{q}$), and the vectors $\mathbf{p}_m$ are chosen to be of the form $\mathbf{p}_m = (m-1)\Delta p \hat{\mathbf{e}}_x$, $m=1,\ldots,M-1$ with $\Delta p = \pi/[(M-1)h]$ and $M=20$. The distance between the measurement planes L is chosen to be equal to the diffuse wavelength $\lambda = 2\pi/k$ ($\lambda \sim 10$ cm *in vivo*), and the field of view of the reconstructed images is $L \times L$. The pixels in the images coincide with the source–detector lattice spacing h.

The dependence of the fundamental limit (in the absence of noise) of transverse resolution on W and h is illustrated in Fig. 1. First, it can be seen that in the case of sufficiently large W and h, the resolution limit is indeed equal to h. For h smaller than a certain value (which depends on W), there is no further improvement in the resolution. For example, for $W=3L$, the resolution limit is achieved at $h \approx L/20$. In the case of an infinite window, the resolution does not improve for $h < L/40$ due to purely computational reasons: The functions K_m, in Eq. (9), decay extremely rapidly with z at the edge of the FBZ, which leads to numerical instabilities. An arrangement, which is practically feasible at the present time, corresponds to $W=2L, L=10h$ (400×400 source–detector pairs). In this case, the resolution achieved is approximately $\lambda/10$. However, significantly higher resolution can be, in principle, achieved with more data.

The resolution in the depth direction is illustrated in Fig. 2. In Fig. 2, we have fixed $h=L/10$ and considered different values of W. In some of the reconstructed images, Gaussian noise of zero mean is added to data at the levels (relative to the mean signal) n as indicated. It can be concluded that for $W=2L$ and $n=1\%$, the resolution is limited by the finiteness of the window rather than by noise. It can be improved by using a larger window ($W=4L$) and simultaneously decreasing ϵ from 10^{-12} to 10^{-15}. At this point, the resolution

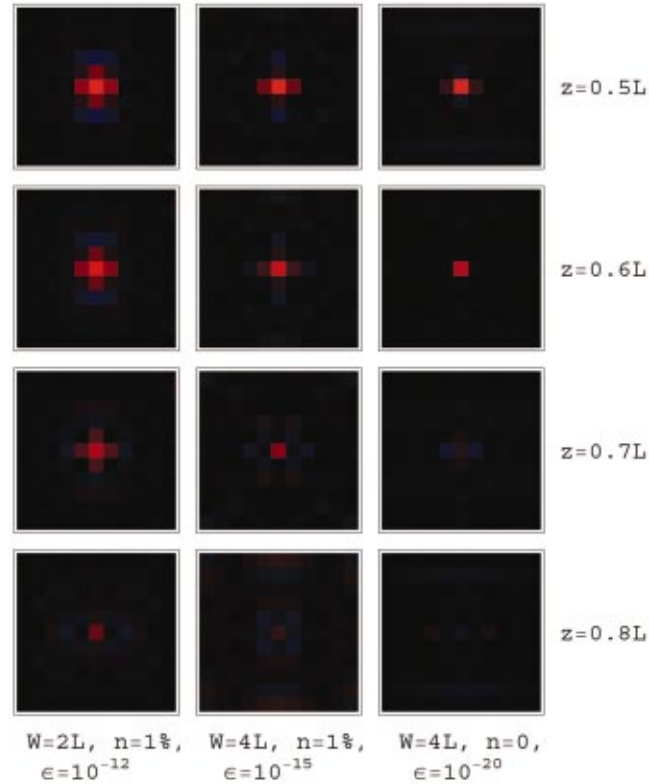

FIG. 2. (Color) Depth resolution for different values of W, levels of noise n, and regularization parameter ϵ.

is controlled by noise, and further increase of W does not lead to any improvement. In the third column, we show the images obtained for the same window size but with $n=0$.

In conclusion, we have studied the transverse and depth resolutions for optical tomography with sampled data. It was found that the fundamental limit of transverse resolution scales as the the transverse separation between nearest sources (detectors) and can be as small as $\lambda/40$.

This research was supported by the NIH.

[1] A. Ishimaru, *Wave Propagation and Scattering in Random Media* (Academic, San Diego, 1978), Vol. 1.
[2] J. B. Fishkin and E. Gratton, J. Opt. Soc. Am. A **10**, 127 (1993).
[3] *Proceedings of Optical Tomography and Spectroscopy of Tissue*, edited by B. Chance, R. R. Alfano, B. J. Tromberg, M. Tamura, and E. M. Sevick-Muraca (SPIE, Bellingham, WA, 2001).
[4] B. W. Pogue, T. O. McBride, U. L. Ostererg, and K. D. Paulsen, Opt. Express **4**, 270 (1999).
[5] J. P. Culver, V. Ntziachristos, M. J. Holboke, and A. G. Yodh, Opt. Lett. **26**, 701 (2001).
[6] F. Natterer, *The Mathematics of Computerized Tomography* (Wiley, New York, 1986).
[7] J. Schotland and J. Leigh, Biophys. J. **61**, 446 (1992).
[8] C. P. Gonatas, M. Ishii, J. S. Leigh, and J. C. Schotland, Phys. Rev. E **52**, 4361 (1995).
[9] V. A. Markel and J. C. Schotland, J. Opt. Soc. Am. A **19**, 558 (2002).
[10] V. A. Markel and J. C. Schotland, Phys. Rev. E **64**, R035601 (2001).
[11] J. C. Schotland and V. A. Markel, J. Opt. Soc. Am. A **18**, 2767 (2001).
[12] P. S. Carney, V. A. Markel, and J. C. Schotland, Phys. Rev. Lett. **86**, 5874 (2001).

Downloaded 12 Aug 2002 to 128.252.91.125. Redistribution subject to AIP license or copyright, see http://ojps.aip.org/aplo/aplcr.jsp